Novel Tandem Quadrupole-Acceleration-Deceleration Mass Spectrometer for Neutralization-Reionization Studies

Frantisek Turecek, Ming Gu, and Scott A. Shaffer
Department of Chemistry, University of Washington, Seattle, Washington, USA

A new tandem mass spectrometer of the quadrupole-acceleration lens-deceleration lens-quadrupole (QADQ) configuration is described. The instrument is designed for neutralization-reionization studies and consists of a 2000-u quadrupole mass analyzer as MS-I, an acceleration electrostatic lens, a series of three differentially pumped collision cells, and an electrostatic deceleration lens, energy filter, and another 2000-u quadrupole mass analyzer as MS-II. The ion optical system achieves high total ion transmission for 5-9-keV ions. Unit mass resolution in neutralization-reionization mass spectra of aromatic compounds is demonstrated. Mass, kinetic energy, and linked scans at various levels of mass resolution and sensitivity are described. *(J Am Soc Mass Spectrom 1992, 3, 493-501)*

Neutralization-reionization mass spectrometry (NRMS) is one of the more recent tandem mass spectrometric techniques [1]. Typically, a beam of mass-selected ions of kiloelectron-volt kinetic energy is allowed to collide with a target gas (Xe, Hg, Na, K, etc.) to undergo electron transfer neutralization [2-6]. The neutrals formed are selected by deflecting away the remaining ions and after several microseconds reionized by collisions with another gas (O_2, NO_2, etc.) [7, 8]. Product ions formed by reionization of neutral fragments or resulting from ion dissociations following reionization are selected by their kinetic energies or momenta and detected to provide a neutralization-reionization (NR) spectrum. NR spectra have been obtained for all four precursor ion-product ion combinations (positive-positive, $^+NR^+$ [1], positive-negative, $^+NR^-$ [9], negative-positive, $^-NR^+$ [10, 11], and negative-negative, $^-NR^-$ [12]) and proved to be highly indicative of ion and neutral structures [1g]. The amount and quality of structural information provided by NRMS is somewhat counterbalanced by the low overall neutralization and reionization efficiencies ($\sim 10^{-4}$) [6]. Neutralization efficiencies (typically 1-20%) [4-7] have been found to depend critically on precursor ion kinetic energy, showing a steep decline below ~ 2 keV [4]. Because of this energy dependence, NRMS has been carried out exclusively on tandem sector mass spectrometers, both commercial [3, 13, 14] and specially designed ones [2, 15].

NR mass spectra obtained at kiloelectron-volt kinetic energies on sector instruments generally show very good reproducibilities, comparable to those achieved in collisionally activated dissociation (CAD) spectra of kileoelectron-volt ions [3]. However, sector instruments of the BE and EBE geometries (B = magnet sector analyzer, E = electrostatic sector analyzer) that employ mass-analyzed kinetic energy (MIKE) scans suffer from low mass resolution due to kinetic energy release in neutral and ion dissociations. This phenomenon is independent of the actual energy resolution achievable with the given instrument, as the fragment ion peak width (in atomic mass units, u) is proportional to the square root of the fragment ion mass, the complementary neutral mass, and the kinetic energy release and inversely proportional to the square root of the precursor ion kinetic energy [16]. The mass resolution problem becomes critical at relatively low masses; for example, an average 13-meV kinetic energy release in the formation of fragments of m/z 142 and 143 from the molecular ion of methyl stearate at 10 keV would leave these fragments unresolved in a MIKE spectrum. Unit or better mass resolution in product ion spectra can be achieved by magnet sector scans (in BEB or EBEB configurations) or by linked B/E scans on BEB, BEEB, or EBEB multisector instruments [17, 18].

An alternative way to solving the mass resolution problem in tandem mass spectrometry relies on using

Address reprint requests to Frantisek Turecek, Department of Chemistry, BG-10, University of Washington, Seattle, WA 98195.

1044-0305/92/$5.00

Received August 26, 1991
Revised November 26, 1991
Accepted December 3, 1991

quadrupole mass analyzers, either in the triple-quadrupole (QQQ) configuration [19] or as sector-quadrupole hybrid instruments (e.g., BEQQ) [20]. Unfortunately, the use of QQQ tandem mass spectrometers for neutralization-reionization studies is hampered by the low neutralization efficiencies in nonresonant electron transfer at low ion kinetic energies [4]. It therefore appeared desirable to design an instrument that would combine the advantages of quadrupole analyzers (good ion transmission, ruggedness, rapid scanning, unit mass resolution, etc.) [21] with the possibility of carrying out ion-neutral and neutral-neutral collisions at high (keV) laboratory kinetic energies. In this article we describe a novel tandem quadrupole mass spectrometer designed for such kiloelectron-volt neutralization-reionization studies.

Design and Construction

The overall instrument design is shown in a block diagram (Scheme I). Precursor ions are formed in an ion source floated at a low (1–100-V) potential and selected by the first quadrupole mass analyzer as MS-I. The ions are accelerated by an ion lens to a kiloelectron-volt kinetic energy and allowed to undergo collisional neutralization and reionization. The reionized precursor and its dissociation products are transported to the deceleration lens, decelerated to low kinetic energies, energy-filtered, and mass-analyzed by the second quadrupole as MS-II. One advantage of such a system is that it achieves effective decoupling of the acceleration and deceleration potentials due to neutral beam transport. The neutral beam potential and kinetic energy is inert to electrostatic potentials applied between the acceleration and deceleration regions (disregarding dipole orientation effects), whereas the reionized ion potential energy is determined by the reionization cell voltage. The reionized ion kinetic energy after deceleration depends on the neutral precursor kinetic energy and the potential difference between the reionization cell and the lens exit element. This means that the latter and all the subsequent focusing devices can be kept at or referenced to the ground potential, avoiding the necessity of floating the MS-II parts and power supplies at high voltage. This greatly simplifies the overall design.

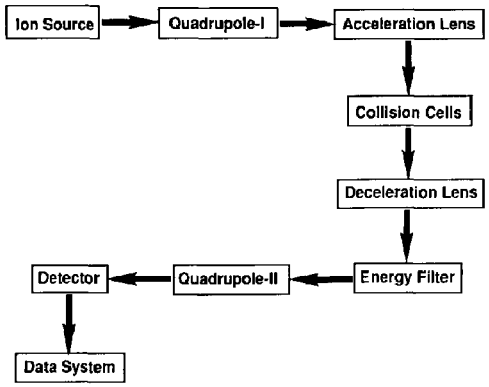

Scheme I

To achieve high transmission through the instrument, the individual components must meet several requirements. First, the acceleration lens ion optics must achieve efficient ion extraction of the divergent ion beam emerging from the first quadrupole analyzer and provide a paraxial beam of kiloelectron-volt ions. Second, the collision cells and the ion transport system must be floated at variable high voltage to allow both precursor ion beam transmission and suppression. Third, the deceleration lens must have good focusing properties at variable retarding potentials in order to allow mass independent fragment ion transmission. Fragment ions formed upon neutralization or reionization have fractional kinetic energies; for example, for fragments of masses m_2 and m_3 formed from a precursor of mass m_1 and kinetic energy T_1, the corresponding kinetic energies (T_2, T_3) are given by eqs 1 and 2.

$$T_2 = \frac{T_1 m_2}{m_1} + \Delta T_2 \quad (1)$$

$$T_3 = \frac{T_1 m_3}{m_1} + \Delta T_3 \quad (2)$$

where the ΔT_2 and ΔT_3 terms include the kinetic energy changes upon neutralization and reionization and kinetic energy release [22]. In order to transmit fragment ions of variable kinetic energies and corresponding m/z values, the deceleration lens voltage must be scanned from the nominal value corresponding to the kinetic energy of the precursor ion to that of the lowest mass fragment. The reionization collision cell is floated at the deceleration lens voltage and thus functions as a reversed ion source. Fast neutrals of kinetic energy T_n reionized in the cell at a given potential, $|U_{dec}|$, will be decelerated to the final ion kinetic energy, $T_i = T_n - |eU_{dec}|$; that is, those of $T_n > |eU_{dec}|$ will pass the deceleration lens, while those of $T_n < |eU_{dec}|$ will be reflected. The deceleration lens thus provides a low mass cutoff that is scanned in link with the second quadrupole analyzer. To filter out high energy ions passing the deceleration lens at $T_i > |eU_{dec}|$, an energy filter must be inserted between the deceleration lens and the second quadrupole analyzer. Finally, the whole ion optical system must be designed so as to match the focusing properties of the acceleration, deceleration, and energy filter lenses, allow for corrections due to mechanical imperfections, and shape the reionized beam to be acceptable for final mass analysis. In the following the individual parts of the tandem QADQ mass spectrometer are described in detail. The potential energy

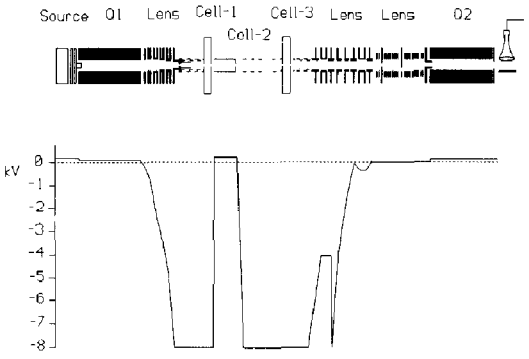

Figure 1. Potential energy profile for transmission of survivor precursor ions following neutralization and reionization.

profile in the acceleration and deceleration regions is shown in Figure 1. All the electrostatic lenses were designed by using the SIMION program [23].

MS-I and Acceleration Lens

The MS-I part consists of an Extrel combined electron and chemical ionization (EI/CI) ion source and an Extrel EXM-2000 quadrupole analyzer (Extrel, Madison, WI) (cylindrical rods, 20.3 cm long, 0.95 cm od) of 2000 u mass range at 1.2 MHz. The ion source voltages and quadrupole dc and radiofrequency (RF) voltages are provided by an Extrel C-60 electronic system. The ion source is mounted on the front ion source housing flange (6-in. ConFlat, 15.24 cm) furnished with power feedthroughs. The ion source support is rotatable along the ion optical axis and spring-loaded to fit into the quadrupole assembly (Figure 2). The assembly is mounted on a plate welded into the opposite (downbeam) 6-in. flange. The ion source housing is furnished with three ports for sample introduction and three additional ports for RF and dc high voltage feedthroughs. The housing is pumped by a 1200 L/s diffusion pump (Varian VHS-4; Varian Associates, Walnut Creek, CA).

The design of the acceleration lens ion optics takes into account the electrostatic field provided by the Extrel exit lens mounted in the quadrupole assembly and maintained at -50 to -150 V. The acceleration lens (Figure 3) is a seven-element cylindrical lens system of gradually diminishing aperture that helps to shape the field lines curvature at different stages of acceleration. Since the trajectories of ions exiting the first quadrupole are unknown due to unknown fringing fields, the acceleration lens was designed to handle a beam of widely different divergence angles and starting x, y coordinates. The lens-focusing properties are shown for such a divergent ion beam (50° full angle, 53 eV nominal kinetic energy) emerging from the quadrupole at variable distances from the optical axis (x, $y = 0$ to ± 5 mm). The quadrupole rods are floated at 38–50 V both to increase the number of cycles the ions undergo while traveling through the analyzer [21] and to facilitate ion extraction from the quadrupole by increasing the voltage difference at the exit. The lens is calculated to produce a convergent beam of 5 mm diameter at the exit plane and half-angle not exceeding 0.8° for the outermost incident rays. For an ion beam of a 50° initial divergence and large off-axis distance, the lens shows large geometric aberrations with ray crossovers at 85–525 mm downbeam from the lens exit plane. However, this is within the acceptance angle and aperture of the deceleration lens (see below). The last lens element carries a quadrupole electrostatic lens floated at the nominal acceleration voltage. The quadrupole lens serves as a full steric angle deflector with the plate voltages being independently adjustable by ± 65 V relative to the nominal high voltage. This allows aiming a 8-keV ion beam at the collision cell entrance aperture for optimum transmittance or deflecting it within $\pm 2.3°$ to study scattering angle effects [24]. The acceleration lens is mounted on a grounded plate that is attached to the vacuum housing 6-in. flange. The high voltage elements are mounted on stainless steel plates stacked on precision alumina insulators (6.35 mm long, 9.5 mm od, 6.35 mm id; McDanel Refractory AP35 Alumina). The plates are centered by four alumina tubes (5.56 mm od, 2.77 mm id) and fastened by stainless steel threaded rods running through the insulator tubes (Figure 4). High voltage is provided by a home-built power supply employing two Bertan 605C-100 modules of 0 to $+10$ kV and 0 to -10 kV variable output for negative and positive ions, respectively. The nominal voltage is distributed to the lens elements by a

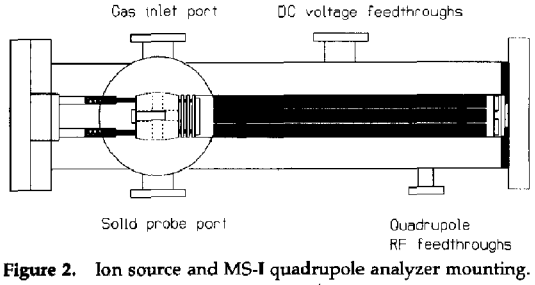

Figure 2. Ion source and MS-I quadrupole analyzer mounting.

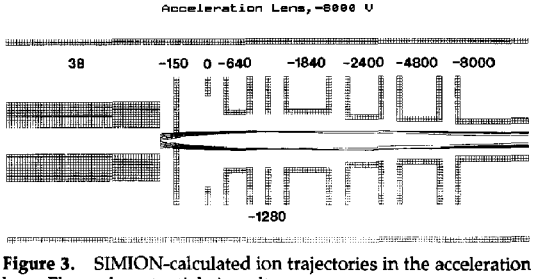

Figure 3. SIMION-calculated ion trajectories in the acceleration lens. Electrode potentials in volts.

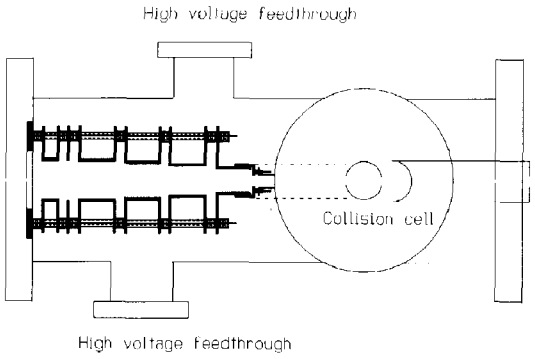

Figure 4. Acceleration lens and neutralization collision cell.

precision voltage divider (Caddock Electronics). The voltages on the first three elements are variable to allow optimum tuning. The quadrupole lens deflector is powered by an American High Voltage module floated at the nominal high voltage.

The accelerated ion beam is transported to the neutralization collision cell through a wide-bore stainless steel screen conduit (25.4 mm id) floated at the nominal high voltage. The neutralization cell is a stainless steel cylinder (20 mm id) mounted vertically on a 4.5-in. (114-mm) flange and insulated by a high voltage break in order to be floated at the nominal acceleration voltage. The neutralization gas is introduced by a fine metering valve and pumped out at the lower end of the collision cell reaching into the intake tube of a 1200-L/s diffusion pump (Varian VHS-4). The ions enter and exit the cell through 5-mm apertures. Ions exiting the neutralization cell are transported through a cylindrical conduit (total length 60 cm) divided into three segments each centered by 95-mm od Teflon disks fitting into the vacuum housing tube and sealed by Viton O-rings. The first segment's front end is shaped to fit the neutralization cell, and the rear end has a 5-mm aperture that serves as a conductance limit between the first and second collision cell (Figure 4). The second segment (length 28 cm, 2.54 cm id) transports the ion beam through the second collision cell (length 15 cm) differentially pumped by a turbomolecular pump (Varian V60, 60 L/s). The third segment transports the ions to the reionization collision cell. These last two segments are made of rolled stainless steel screen and are spaced 6 cm apart. This gap works as a symmetrical two-element lens that refocuses the outermost divergent rays and improves ion transmission. The segments can be independently floated at variable potentials. Typically, in the ion transmission mode all three segments are maintained at the nominal acceleration or deceleration voltage. In the $^{+}NR^{+}$ mode the first segment is floated at +120 V to deflect the precursor ions following neutralization. Alternatively, floating both the second and third segments at the deceleration potential or grounding the second segment and floating the third one allows for variable reionization collisional paths. Note that ions formed by collisional reionization of kiloelectron-volt neutrals at ground potential will retain their high kinetic energies after passing the deceleration lens and eventually be filtered out (see below). However, thermal gas molecules that are ionized by neutral beam impact in the field gradient between the conduit segments can be detected (see below). Ions and neutrals are led through the high voltage floated conduit to the reionization collision cell also floated at the deceleration voltage. The reionization cell is constructed and mounted identically as the neutralization cell and is differentially pumped by a 1200-L/s diffusion pump (Varian VHS-4; Figure 5).

Deceleration Lens and MS-II

The deceleration lens was designed according to Schlunegger and co-workers [25]. This combines decelerating stages with refocusing einzel lens elements to compensate for the increased divergence upon deceleration [26]. According to ion trajectory calculations (Figure 6), a slightly divergent (0.3° half-angle) 8053-eV ion beam entering the lens is decelerated to 53 eV and refocused to a convergent beam of < 0.44° half-angle. In the NR mode the potentials at the first five elements are proportionately scanned to allow for the fractional kinetic energies of product ions (see above). The ion trajectories should be independent of the absolute electrostatic potentials, provided that the voltage ratios remain constant during the scan [26]. The last einzel lens element (−250 V) is a kept at a constant voltage that is tuned for optimum beam transmission. SIMION calculations show very similar exit trajectories for 53-eV ions decelerated from kinetic energies in the range of 1-10 keV, indicating negligible kinetic energy and mass discrimination in the deceleration step. High voltage for the deceleration lens is provided by a Spellman RHR programmable power supply of reversible polarity (0 to ±10 kV).

Other lens designs (e.g., the exponential retarding lens [27, 28] and that of Allison and co-workers [29]) have been analyzed and appeared to be less suitable for decelerating ions in the 8-10-keV range. In the

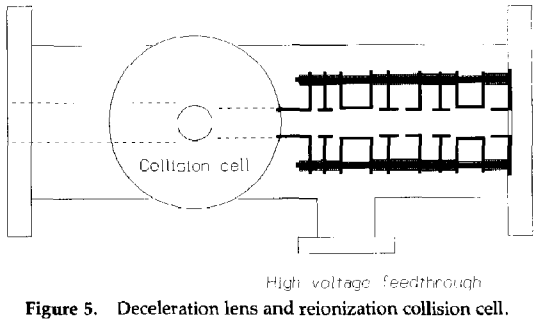

Figure 5. Deceleration lens and reionization collision cell.

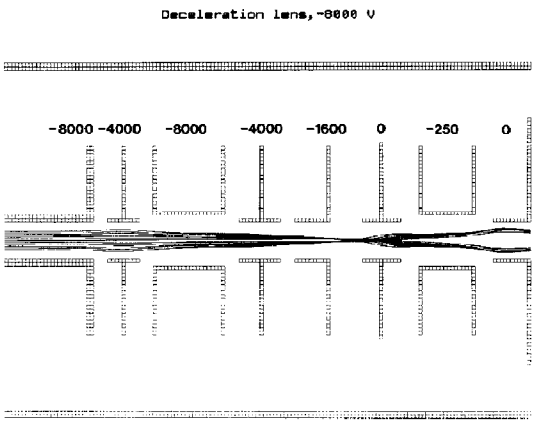

Figure 6. SIMION-calculated ion trajectories in the deceleration lens. Electrode potentials in volts.

Allison design a paraxial ion beam is focused by an einzel lens prior to the deceleration stage, finally producing a slightly divergent beam (< 3° half-angle for 3-keV ions) [29]. Our SIMION calculations find that this divergence angle increases with increasing precursor ion kinetic energy, and the decelerated ion trajectories become sensitive to the fast beam divergence angle. For example, decelerating 10-keV ion beam of 0.3° half-angle divergence is calculated to produce 50-eV ions of 9.3° half-angle divergence. This would require further refocusing to make the ion beam acceptable for the energy filter.

The decelerated ion beam enters an energy filter chicane lens consisting of four sets of deflector plate electrodes of opposite polarities symmetrically positioned about a grounded central stop blocking the optical axis (Figure 7). According to ion trajectory calculations, the filter has an energy bandwidth of ~25 eV for a paraxial ion beam. The energy bandwidth was calculated to be quite sensitive to the entering ion trajectories. For example, at 2° oblique entrance angle, the bandwidth increases to ~50 eV, and similar effects are calculated for nonparaxial entering ions. The ion beam is compressed in the region of the optical stop, which improves overall ion transmission. The optical stop is mounted on a precision linear motion feedthrough that allows its vertical position to be changed within 2.5 cm. The energy filter lens is further furnished with two pairs of vertical and horizontal deflector electrodes that allow the entering and exiting ion beam to be positioned and focused. This is shown in the ion trajectory calculations (Figure 7) where the divergent 53-eV ion beam exiting the energy filter lens at the ground potential plate is refocused by applying −15 V on the deflector electrodes and +45 V on the quadrupole entrance lens plate. With the exception of the optical stop, the energy filter lens plates are stacked on precision ceramic insulators and mounted on the quadrupole analyzer assembly. The assembly consists of another Extrel EXM-2000 mass filter with entrance and exit lenses, an off-axis CEM detector (Galileo Channeltron 4870), and a conversion dynode charged up to a −4.06 kV. The quadrupole analyzer assembly is mounted on the rear end 6-in. flange furnished with RF and dc voltage feedthroughs. This part of the instrument is differentially pumped by another Varian V60 turbomolecular pump. The quadrupole analyzer RF and dc power and control are provided by an Extrel C-50 electronic system. DC voltages to the energy filter lens, deflectors, and the quadrupole entrance and exit lenses are provided by voltage dividers powered by two Lambda LQD-423 regulated power supplies.

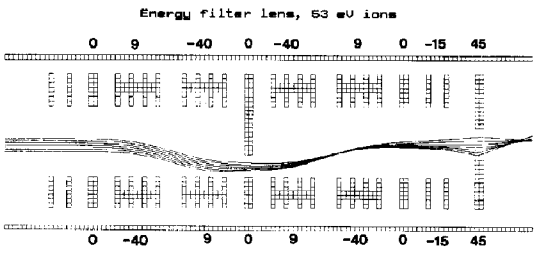

Figure 7. SIMION-calculated ion trajectories in the energy filter lens.

The electron current output from the multiplier is converted to voltage by a Keithley 428 amplifier (10^{11} V/A maximum gain) and handled by a PC-based data acquisition system that allows digital signal averaging, smoothing, peak area integration, and mass scale corrections and also provides scan control [30]. The scanning voltage ramp (0–10 V) is provided by a 16-bit digital-to-analog converter (Burr-Brown PCI-20006M-2) also used to drive both the dc high voltage and the quadrupole power supplies.

Ion Beam Transmission

The major objectives of the QADQ design are a high ion transmission through the instrument and unit mass resolution in precursor ion selection and product ion analysis following high energy collisions. These features have been tested in the first experiments following instrument construction. To determine ion transmittance, one would need to measure total currents of ions entering and exiting the ion optical system. However, this would require significant modifications in both the ion source and detector regions, so we resorted to estimating the ion transmittance on the basis of the measurable electron currents as follows. Acetone was introduced into the ion source housing from a port remote from the ion source to read 2.5×10^{-6} torr on an Bayard-Alpert ionization gauge located near the ion source block and calibrated to nitrogen. This corresponds to 1×10^{-6} torr or 3.54×10^{10} acetone molecules/cm^3 in the ionization

volume [31]. The total electron emission current was adjusted to 0.25 mA at 70 eV. Since the Extrel ion source uses a dual-filament system without electron trap current stabilization, the fraction of electrons entering the ionization volume had to be estimated. This was done by SIMION calculations that gave an average 25% electron transmission (0.062 mA effective ionizing current). Combining this with the acetone number density, ionization cross section (9.0×10^{-16} cm^2) [32] and the ionization volume dimensions, we calculated 2×10^{-9} A of ions being formed. SIMION ion trajectories based on the calculated ion source potentials showed that about 25% of the primary ions formed in the ionization volume left the ion source, out of which another 20% fraction followed highly divergent trajectories. Hence we estimated that about 20% of the total ions formed (4×10^{-10} A) can be extracted and refocused to enter the MS-I quadrupole analyzer. The MS-I and MS-II mass analyzers were set to the RF-only mode, and all the focusing voltages were adjusted to maximize the total ion current. The multiplier gain (at 1.35 kV, conversion dynode off) was estimated to be 1×10^5 [33], giving 0.94 V output voltage with 10^5 amplifier gain. This corresponds to 9.4×10^{-11} A of total ion current arriving at the detector. Hence the total ion transmission was calculated as 23%, although it should be emphasized that this is a very crude estimate, as also pointed out by a referee.

From the computed ion trajectories it appears that most of the transmission loss observed occurs in the fringing field at the MS-I quadrupole analyzer exit [34]. By contrast, the energy filter lens shows negligible transmission loss; for example, lifting the optical stop and reoptimizing the electrode potentials resulted in no transmission gain (±5%). In the energy filter mode, intercepting the ion beam with the optical stop gave beam width of 1.1 mm, very close to that predicted from ion trajectory calculations (1.13 mm). The overall ion transmission (without neutralization and reionization) is very little sensitive to exact matching of the acceleration and deceleration voltages; for example, changes by ±100 V result in 5–10% beam intensity variations at 8 keV. By contrast, ion transmission after neutralization-reionization depends critically on the adjustment of the acceleration and deceleration lens voltages. The instrument maintains high transmission down to 4 keV after retuning the acceleration lens and deflector potentials. By contrast, ion trajectory calculations (carried out for 53-eV ions of 50° full angle divergence; see above) predict significant increase of the beam width upon decreasing the acceleration voltage (e.g., by 45% from 10 to 5 keV), suggesting a twofold decrease in overall transmission due to the limited apertures size. The essentially unchanged transmission at 4–10 keV indicates that ions of much lower divergence are in fact extracted from the MS-I quadrupole analyzer.

Operating the quadrupole analyzers in the mass-selective mode decreases ion transmission, depending on the selected peak width [21]. The transmission loss was measured with $CH_3I^{+\cdot}$ at m/z 142 by selecting the ion with one quadrupole analyzer at low mass resolution, Δm = 1.5 u (full width at half maximum, fwhm), and varying the dc/RF voltage ratio at the other analyzer. Typically, the I(RF-only)/I(Δm) intensity ratios were 1.2, 2.4, and 4.5 for Δm(fwhm) equal to 1.5, 0.7, and 0.4 (unit mass resolution, 10% valley) u, respectively. Hence with both quadrupole analyzers at unit mass resolution, the total ion transmission is 1.1% at maximum.

NRMS with a QADQ Mass Spectrometer

A series of tests were performed to assess QADQ performance in the neutralization-reionization mode. NRMS spectra of methyl iodide were obtained with the precursor ion accelerated to 8 keV kinetic energy, Xe (at 70% incident beam transmittance, T) as the neutralization reagent, and O_2 (70% T) as the reionization gas. The first and second ion conduit segments were floated at 120 V to reflect the primary ion beam after passing the neutralization cell. Interestingly, a small residual ion current persisted at conduit voltages < 105 V despite the 53-eV nominal ion kinetic energy (for a detailed discussion of ion kinetic energies upon leaving the ion source, see ref 29). We attribute this residual current to a small fraction of doubly charged ions (CH_3I^{2+} and I^{2+}) formed in the ion source and gaining 106 eV kinetic energy upon exiting the ion source. $^+NR^+$ mass spectra were taken with different combinations of MS-I and MS-II quadrupole settings. With MS-I set to pass m/z 142 and MS-II set to the RF-only mode while scanning the deceleration voltage (D scan), one obtains a kinetic energy spectrum (Figure 8a) analogous to an HV scan on a sector instrument [16]. Note the low m/z 142: m/z

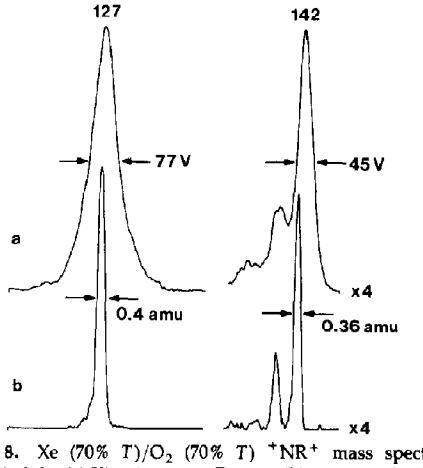

Figure 8. Xe (70% T)/O_2 (70% T) $^+NR^+$ mass spectra of methyl iodide. (a) Kinetic energy D scan; (b) mass-resolved D/Q scan.

127 abundance ratio compared to that in the 70-eV electron impact mass spectrum of methyl iodide. The peak of the I^+ fragment is substantially broader (ΔT = 77 V fwhm) than that of $CH_3I^{+\cdot}$ (45 V fwhm). The latter value is largely determined by the energy bandwidth of the filter lens (see above), whereas the greater I^+ peak width can be accounted for by ~85-meV kinetic energy release in CH_3I neutral or ion fragmentation (or both) [16]. With the MS-II quadrupole analyzer being set at unit mass resolution (10% valley in the EI mass spectrum) and scanned with the deceleration voltage (D/Q linked scan), the $^+NR^+$ mass spectrum of $CH_3I^{+\cdot}$ shows baseline resolved peaks (< 1% valley; Figure 8b). The D/Q scan mode is analogous to the B/E linked scan with previous mass selection as employed on triple-sector instruments of the BEB geometry [18]. The peak width (fwhm) is essentially constant (0.36–0.4 u) for reionized $CH_3I^{+\cdot}$, CH_2I^+, and I^+. The integrated relative intensities of I^+ and ($CHI^{+\cdot}$ + CH_2I^+ + $CH_3I^{+\cdot}$) differ somewhat for the D and D/Q scans (84/16% and 80/20%, respectively) due to the narrower bandwidth of the mass analyzer, which discriminates against the broader I^+ peak. The mass-resolved $^+NR^+$ mass spectrum of $CH_3I^{+\cdot}$ did not change upon setting the MS-I quadrupole to the RF-only mode and tuning to maximum ion transmission, whereas overall NR sensitivity increased 4–5 times. Unless unit mass resolution in MS-I separation is required, this is the preferred scan mode, combining unit MS-II mass resolution with high MS-I ion transmission. This is also analogous to a B/E linked scan on a sector instrument [18].

The neutralization and reionization collision cells of the QADQ instrument are substantially farther apart (60 cm) than those on commercial or home-built sector tandem instruments [13–15], and also the acceptance angle of the QADQ is greater than that of a sector instrument. This could presumably result in more extensive fragmentation due to the longer neutral path length and dissociation time scale and enhanced collection of fragments formed at larger scattering angles [24]. However, direct comparison of NR mass spectra obtained on instruments of such different designs is difficult because of different discrimination factors. Thus low kinetic energy (and low mass) fragment ions are discriminated on sector mass spectrometers, whereas high mass (precursor) ions can be discriminated on quadrupole instruments [18]. The $^+NR^+$ mass spectrum of benzene measured on the QADQ instrument showed slightly lower survivor $C_6H_6^{+\cdot}$ relative abundance (19.2% of the total reionized ion current) than reported for a spectrum obtained on a sector instrument (22.7%) [6]. The total $^+NR^+$ efficiency of $C_6H_6^{+\cdot}$ (1.0×10^{-4}) obtained *at unit product ion mass resolution* is comparable to that reported for a $^+NR^+$ spectrum measured on a sector instrument (1.02×10^{-4}) at somewhat higher beam transmittance (Xe, 85% T/O_2, 90% T) [6].

The NR efficiency can be increased by using a different neutralization target [6]. With benzene neutralization we find methyl iodide to be 2.5 times more efficient than xenon, possibly because of the closer match of the $C_6H_6^{+\cdot}$ recombination energy and CH_3I ionization energy (9.54 eV) and the greater polarizability of CH_3I (7.97×10^{-24} cm^3) [35] compared to that of xenon (4.04×10^{-24} cm^3) [36].

Xe/O_2 $^+NR^+$ mass spectra of phenol [37] were measured in different MS-I and MS-II modes (Figure 9). With the MS-II in the mass selective mode, the $^+NR^+$ spectra obtained by D/Q linked scan were essentially independent of whether the phenol molecular ion was mass-selected by MS-I or whether the latter was set to the RF-only mode (Figure 9a). A D/Q scan with the MS-II quadrupole analyzer in the RF-only mode of mass-selected $C_6H_5OH^{+\cdot}$ (Figure 9b) shows low mass resolution and strong bias toward low mass fragments. This results from the changing ion transmission through the analyzer as the low mass setting is scanned toward higher m/z values. Mass resolution further degrades upon setting the MS-I quadrupole to the RF-only mode in order to pass all primary ions, while MS-II is scanned in the D/Q mode with the quadrupole analyzer in the RF-only mode (Figure 9d). This still provides limited mass

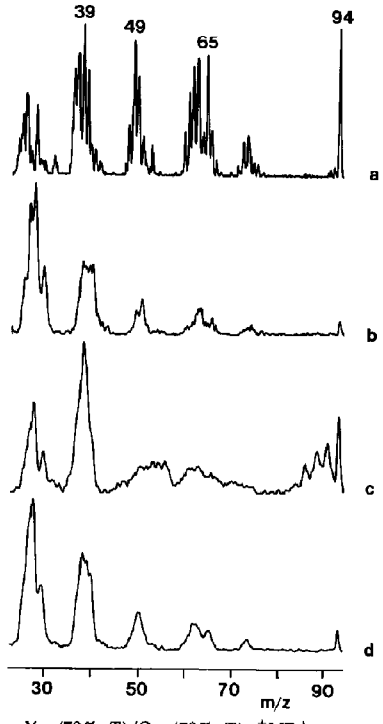

Figure 9. Xe (70% T)/O_2 (70% T) $^+NR^+$ mass spectra of phenol. (**a**) Mass-resolved D/Q scan; (**b**) D/Q-RF-only scan of mass-selected $C_6H_5OH^+$; (**c**) mass-unresolved D scan; (**d**) mass-unresolved D/Q-RF-only scan. The small peak at m/z 32 is due to ionization of oxygen between the ion conduit segments.

analysis at the MS-II stage at enhanced sensitivity, as the quadrupole analyzer passes ions of m/z greater than 7/9 of the given mass setting. Finally, fixing both quadrupole analyzers in the RF-only mode and scanning the decelerating voltage provides a mass-unresolved spectrum (Figure 9c) analogous to an ion kinetic energy scan on a sector instrument of an EB geometry [16].

Low mass resolution in kinetic energy scans is especially critical with NR mass spectra of aromatic ions whose dissociations are accompanied by large kinetic energy release [37, 38] or at higher m/z where important product ions can be unresolved and escape detection [39]. The importance of sufficient mass resolution for correct m/z assignment and abundance measurements is illustrated by the m/z 60–66 region in the $^{+}NR^{+}$ mass spectrum of phenol (Figure 10). The mass-resolved spectrum [Xe (70% T)/O_2 (70% T), average of five scans, top] allows unambiguous assignment of fragment m/z values. The NR mass spectrum obtained on a sector instrument by averaging 30 kinetic energy scans (Figure 10, bottom) [37] would require deconvolution to yield m/z and intensity information. Unit mass resolution in NR mass spectra of deuterium-labeled aromatic compounds has been achieved by B/E linked scan on an EBEB tandem sector mass spectrometer [40].

The preliminary results reported above allow us to conclude that the QADQ mass spectrometer is suitable for neutralization-reionization studies and offers several advantages over BE and EBE sector instruments. In addition to the features discussed above, the overall equipment cost ($130,000) compares favorably with that of commercial instruments.

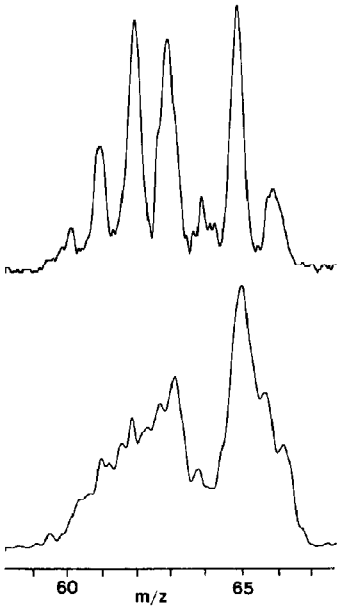

Figure 10. Region of m/z 60–66 in the $^{+}NR^{+}$ mass spectrum of phenol. Top: mass resolved D/Q scan. Bottom: ESA scan [37].

Acknowledgments

Financial support by the University of Washington Graduate School Fund, National Science Foundation (Grant CHE-9102442) and Center for Process Analytical Chemistry at the University of Washington is gratefully acknowledged. Acknowledgment is also made to the donors of the Petroleum Research Fund, administered by the ACS, for partial support of this work.

References

1. (a) Gellene, G. I.; Porter, R. F. *Acc. Chem. Res.* **1983**, *16*, 200. (b) Wesdemiotis, C.; McLafferty, F. W. *Chem. Rev.* **1987**, *87*, 485. (c) Terlouw, J. K.; Schwarz, H. *Angew. Chem. Int. Ed. Engl.* **1987**, *26*, 805. (d) Holmes, J. L. *Adv. Mass Spectrom.* **1989**, *11*, 53. (e) Terlouw, J. K. *Adv. Mass Spectrom.* **1989**, *11*, 984. (f) Holmes, J. L. *Mass Spectrom. Rev.* **1989**, *8*, 513. (g) McLafferty, F. W. *Science* **1990**, *247*, 925.
2. Gellene, G. I.; Porter, R. F. *J. Chem. Phys.* **1984**, *81*, 5570.
3. Terlouw, J. K.; Kieskamp, W. M.; Holmes, J. L.; Mommers, A. A.; Burgers, P. C. *Int. J. Mass Spectrom. Ion Proc.* **1985**, *64*, 245.
4. Danis, P. O.; Feng, R.; McLafferty, F. W. *Anal. Chem.* **1986**, *58*, 348.
5. Burgers, P. C.; Kulik, W.; Versluis, C.; Terlouw, J. K. *Int. J. Mass Spectrom. Ion Proc.* **1990**, *98*, 247.
6. Hop, C. E. C. A.; Holmes, J. L. *Org. Mass Spectrom.* **1991**, *26*, 476.
7. Gellene, G. I.; Porter, R. F. *Int. J. Mass Spectrom. Ion Proc.* **1985**, *64*, 55.
8. Danis, P. O.; Feng, R.; McLafferty, F. W. *Anal. Chem.* **1986**, *58*, 355.
9. Feng, R.; Wesdemiotis, C.; McLafferty, F. W. *J. Am. Chem. Soc.* **1987**, *109*, 6521.
10. Bowie, J. H.; Blumenthal, T. *J. Am. Chem. Soc.* **1975**, *97*, 2959.
11. Mercer, R. S.; Harrison, A. G. *Org. Mass Spectrom.* **1987**, *22*, 710.
12. McMahon, A. W.; Chowdhury, S. K.; Harrison, A. G. *Org. Mass Spectrom.* **1989**, *24*, 620.
13. Harrison, A. G.; Mercer, R. S.; Reiner, E. J.; Young, A. B.; Boyd, R. K.; March, R. E.; Porter, C. J. *Int. J. Mass Spectrom. Ion Proc.* **1986**, *74*, 13.
14. Wesdemiotis, C.; Polce, M. J.; Bott, P. A.; Bordoli, R. S. *Proceedings of the 38th ASMS Conference on Mass Spectrometry and Allied Topics*, Tucson, AZ, 1990, pp 1132–1133.
15. Feng, R.; Wesdemiotis, C.; Baldwin, M. A.; McLafferty, F. W. *Int. J. Mass Spectrom. Ion Proc.* **1988**, *86*, 95.
16. Cooks, R. G.; Beynon, J. H.; Caprioli, R. M.; Lester, G. R. *Metastable Ions*; Elsevier: Amsterdam, 1973.
17. (a) McLafferty, F. W.; Todd, P. J.; McGilvery, D. C.; Baldwin, M. A. *J. Am. Chem. Soc.* **1980**, *102*, 3360. (b) Boerboom, A. J. H. *Rapid Commun. Mass Spectrom.* **1990**, *4*, 385.
18. (a) McLafferty, F. W., Ed. *Tandem Mass Spectrometry*. Wiley: New York, 1983. (b) Busch, K. L.; Glish, G. L.; McLuckey, S. A. *Mass Spectrometry/Mass Spectrometry: Techniques and Applications of Tandem Mass Spectrometry*; VCH Publishers: New York, 1988, pp 22–34.
19. Yost, R. A.; Enke, C. G. *J. Am. Chem .Soc.* **1978**, *100*, 2274.
20. Glish, G. L.; McLuckey, S. A.; Ridley, T. Y.; Cooks, R. G. *Int. J. Mass Spectrom. Ion Proc.* **1982**, *41*, 157.
21. Dawson, P. H. *Mass Spectrom. Rev.* **1986**, *5*, 1.

22. Bordas-Nagy, J.; Holmes, J. L.; Hop, C. E. C. A. *Int. J. Mass Spectrom. Ion Proc.* **1989**, *94*, 189.
23. Dahl, D. A.; Delmore, J. E. *The SIMION PC/PS2 User's Manual, Version 4.0.* Publication no. EGG-CS-72333, Rev. 2. U.S. Department of Energy: Washington, DC, 1988.
24. Fura, A.; Turecek, F.; McLafferty, F. W. *J. Am. Soc. Mass Spectrom.* **1991**, *2*, 492.
25. Kofel, P.; Reinhard, H.; Schlunegger, U. *Org. Mass Spectrom.* **1991**, *26*, 463.
26. Paszkowski, B. *Electron Optics*; Illiffe Books: London, 1968, p 163.
27. Vestal, M. L.; Blakley, C. R.; Ryan, P. W.; Futrell, J. H. *Rev. Sci. Instrum.* **1976**, *47*, 15.
28. Lindholm, E. *Rev. Sci. Instrum.* **1960**, *31*, 210.
29. O'Connor, P. J.; Leroi, G. E.; Allison, J. *J. Am. Soc. Mass Spectrom.* **1991**, *2*, 322.
30. Drinkwater, D. E.; Turecek, F.; McLafferty, F. W. *Org. Mass Spectrom.* **1991**, *26*, 559.
31. Bartmess, J. E.; Georgiadis, R. M. *Vacuum* **1983**, *33*, 149.
32. Fitch, W. L.; Sauter, A. D. *Anal. Chem.* **1983**, *55*, 832.
33. Kurz, E. A. *Amer. Lab.* **1979**, *11*, 67.
34. Dawson, P. H. *Int. J. Mass Spectrom. Ion Proc.* **1990**, *100*, 41.
35. Lide, D. R., Ed. *CRC Handbook of Chemistry and Physics*, 71st ed.; CRC Press: Boca Raton, FL, 1990, pp 10–203.
36. Miller, T. M.; Bederson, B. *Adv. At. Mol. Phys.* **1977**, *13*, 1.
37. Turecek, F.; Drinkwater, D. E.; Maquestiau, A.; McLafferty, F. W. *Org. Mass Spectrom.* **1989**, *24*, 669.
38. Maquestiau, A.; Flammang, R.; Plisnier, M.; Wentrup, C.; Kambouris, P.; Paton, M. R.; Terlouw, J. K. *Int. J. Mass Spectrom. Ion Proc.* **1990**, *100*, 477.
39. Weiske, T.; Böhme, D. K.; Hrušák, J.; Krätschmer, W.; Schwarz, H. *Angew. Chem. Int. Ed. Engl.* **1991**, *30*, 884, and references therein.
40. Drinkwater, D. E.; McLafferty, F. W.; private communication, August 1991.